Available online at www.sciencedirect.com

ScienceDirect

Electronic Notes in Theoretical Computer Science 296 (2013) 27–42

Electronic Notes in Theoretical Computer Science

www.elsevier.com/locate/entcs

A Structured Stochastic Model for Prediction of Geological Stratal Stacking Patterns

Joaquim Assunção [1] Luciana Espindola [1] Paulo Fernandes [1,2,3]
Maria Pivel [1] Afonso Sales

Pontifícia Universidade Católica do Rio Grande do Sul
Avenida Ipiranga, 6681 – Prédio 32
90619-900 – Porto Alegre – RS – Brazil
Tel.: +55-51-3320-3611
Fax: +55-51-3320-3621

Abstract

This article presents a novel *Stochastic Automata Networks* (SAN) model to estimate the behavior of sediment strata formation in continental margins resulting from interaction between sea level, sediment input and subsidence over the last 130 million years. The model result is a set of probabilities that can be compared with geological facts and hypothesis; thus, we can point out possible discrepancies from other similar works and also improve the chance of a good estimation of past geological events.

Keywords: Performance Evaluation, Analytical Modeling, Stochastic Automata Networks

1 Indroduction

The present study describes a novel application of *Stochastic Automata Networks* (SAN) [1,2,3] to model a specific type of geological phenomenon. This is a challenging subject, provided that most of the natural phenomena depend on a great number of factors to explain their evolution. Due to such a large number of natural variables, one of the most important steps in the modeling activity is the selection, discretization and grouping of the most significant variables to the phenomenon considered.

[3] *Email:* joaquim.assuncao@pucrs.br (Joaquim Assunção), luciana.espindola@acad.pucrs.br (Luciana Espindola), paulo.fernandes@pucrs.br (Paulo Fernandes), maria.pivel@pucrs.br (Maria Pivel), afonso.sales@pucrs.br (Afonso Sales)

[1] Authors received financial support provided by PUCRS-Petrobras (Conv. 0050.0048664.09.9).

[2] Paulo Fernandes is also funded by CNPq-Brazil (PQ 307284/2010-7).

[3] Corresponding author. The order of authors is merely alphabetical.

1571-0661/$ – see front matter
http://dx.doi.org/10.1016/j.entcs.2013.07.003

This study shows a first attempt to represent the evolution of a sedimentary basin using the SAN formalism. Pelotas basin, located in southernmost Brazil (Figure 1), was the basin chosen to attend this purpose. Considerable amounts of information are available for this marginal basin, including stratigraphic architecture (Figure 2), changes in sediment yield, and subsidence. Most of the information from Pelotas basin used in this paper is extracted from Contreras *et al.* [4].

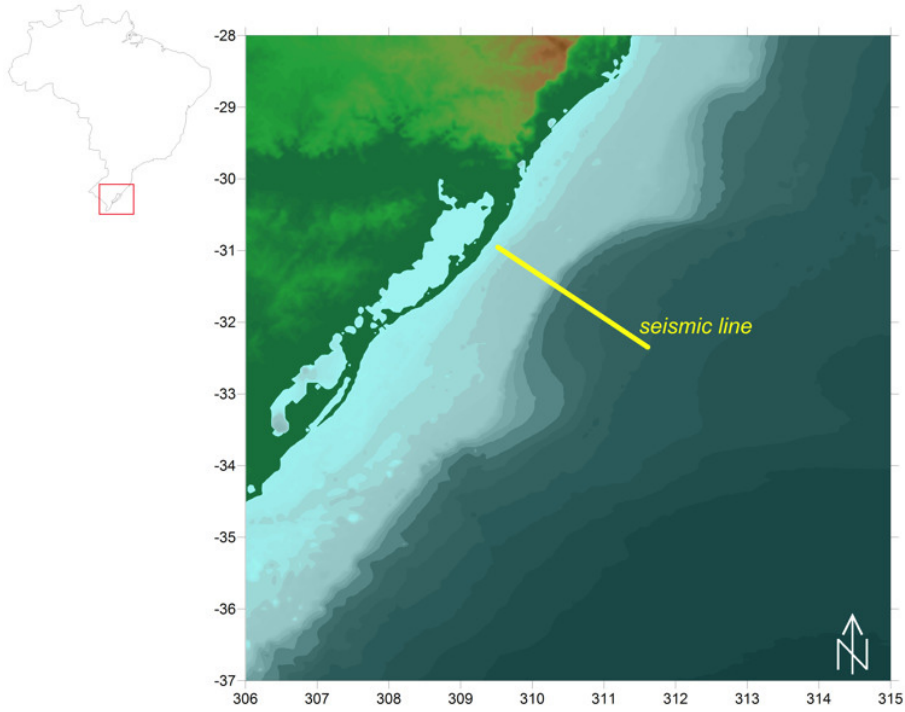

Fig. 1. Location of Pelotas basin in southern Brazil, and seismic line analyzed by Contreras *et al.*, [4].

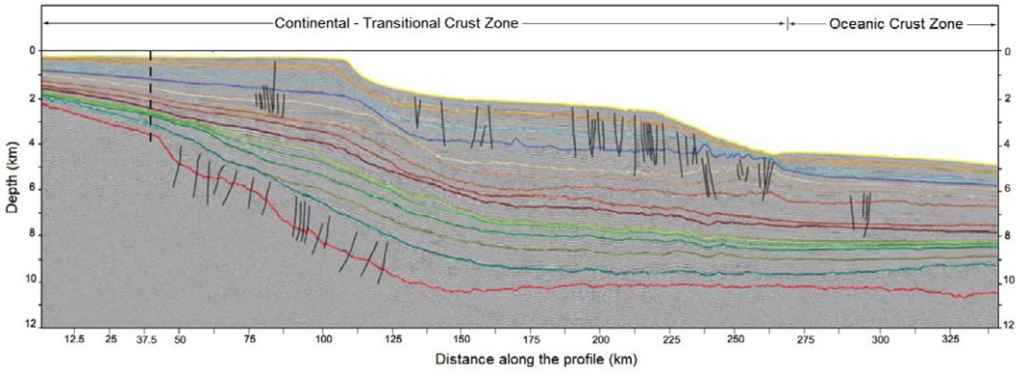

Fig. 2. Interpreted seismic reflection profile from Pelotas basin [4]. In seismic reflection surveys, the measurement of the time required for a seismic wave or pulse to return to the surface after reflection from subsurface interfaces of different physical properties provides information on the arrangement of sedimentary strata. Color lines depict reflectors from different ages. Vertical exaggeration 8:1.

This article is organized as follows: Section 2 provides the necessary background

on the geological phenomena, favouring the model comprehension; Section 3 concisely describes the SAN formalism; Section 4 is dedicated to describing the proposed SAN model for Pelotas basin; Section 5 presents the experiment conducted and the results achieved; and Section 6 is dedicated to discuss the model and confront the results with the expected from geological standpoint.

2 Geology Background

Sedimentary basins constitute large accumulations of sediments. The amounts and types of sediments depend on factors such as climate and relief, and for this reason, sedimentary basins constitute essential records of the climatic and tectonic history of the Earth.

The study of sedimentary basins is primarily based on drilling and seismic surveys, which provide information on the composition and arrangement of sedimentary rock strata. The configuration of strata results from the interplay between sediment supply and relative base level changes, which defines the accommodation space for those sediments. In marginal sedimentary basins, *i.e.*, basins along a continental margin, the base level is determined by the relative sea level, which, in turn depends on the global (*eustatic*) sea level changes and on the vertical movement of the underlying crust (Figure 3). Crustal movement can be either upwards (*uplift*) or downwards (*subsidence*).

Four genetic types of deposit can be distinguished as a function of relative sea level changes, as summarized in Figure 4 (a). These are named forced regression (FR), lowstand normal regression (LNR), highstand normal regression (HNR), and transgression (T). Forced regressions occur whenever relative sea level falls. During these events, sediments prograde seawards and the shoreline advances with downstepping (Figure 4 (b)). Normal regressions occur whenever sea level is rising but sedimentation rate outpaces the rate of sea-level rise, avoiding shoreline retreat. Normal regressions may either occur during a relative sea level lowstand or highstand. During lowstands, there is an acceleration of sea level rise and the rate of progradation decreases with time while the rate of vertical accretion (known as *aggradation*) increases with time (Figure 4 (c)). Conversely, as sea level decelerates at the end of a sea-level rise trend, there is a decrease in the rate of aggradation with time and an increase in progradation (Figure 4 (c)). Finally, transgressions occur when the rate of sea level rise is the highest and the sediment supply is not enough to compensate for it. During transgressions, the shoreline retreats as the sea advances over the continent and sediments accumulate progressively landwards, in a configuration known as *retrogradation* (Figure 4 (d)).

Clearly, the simplified model in Figure 4 does not represent the whole complexity of processes that may affect the configuration of sedimentary strata such as variable sediment supply and shelf gradient. Nevertheless, it emphasizes the dominant role of relative-sea level changes and provides a clear picture of the main processes and possible stratigraphic architectures.

Contreras *et al.* [4] estimated subsidence rates and sediment flux using numer-

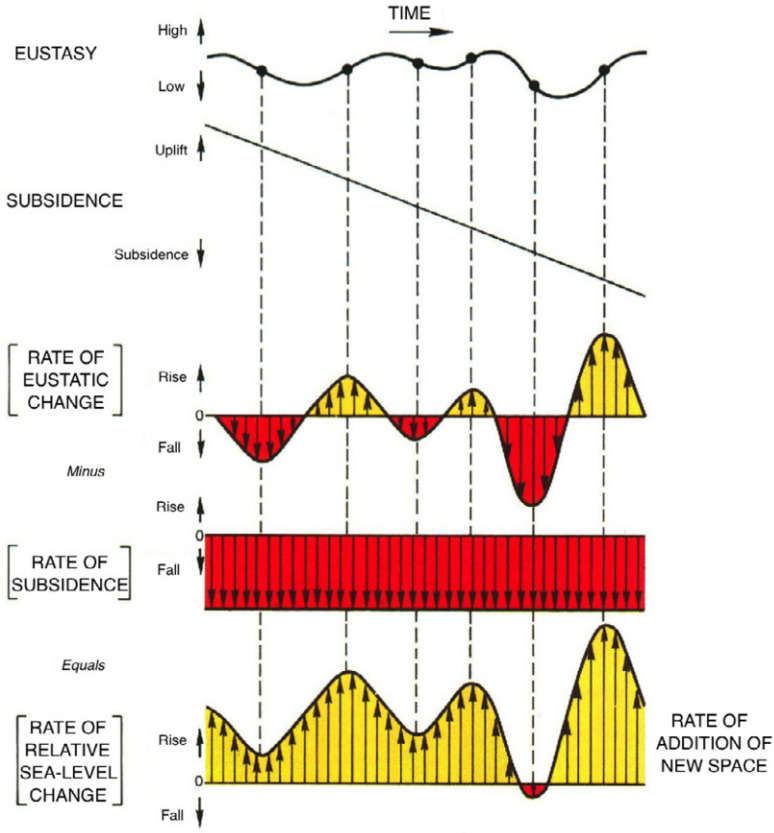

Fig. 3. Rate of relative sea level change and addition of new accommodation space as a function of eustatic (global) sea level changes and subsidence [5].

ical modeling (Figure 5). These estimates were obtained considering the eustatic (global) sea level curve proposed by Hardenbol *et al.* [8] re-calibrated to a more recent geological timescale [9], as plotted in Figure 6. Higher order, *i.e.*, higher frequency, sea-level changes were excluded from the analysis because of the lower resolution of the seismo-stratigraphic data (2nd order depositional units, 3-50 Ma), their less defined amplitudes and partly disputed eustatic origin [10].

3 Stochastic Automata Networks

When a stochastic process has many states its representation by an ordinary Markov chain may be confuse or difficult to handle. In such cases, the use of a structured formalism as, for instance, *Stochastic Automata Networks* (SAN) [1,3] may cope the problem.

A first step when using SAN as a modeling tool is to identify structures within the process. Each structure is treated as an automaton, composed of states and transitions. Every single transition is ruled by one or more events, which are classified as local or synchronizing. A local event operates over only one automaton, changing its state by triggering a transition without interfering on the other automata

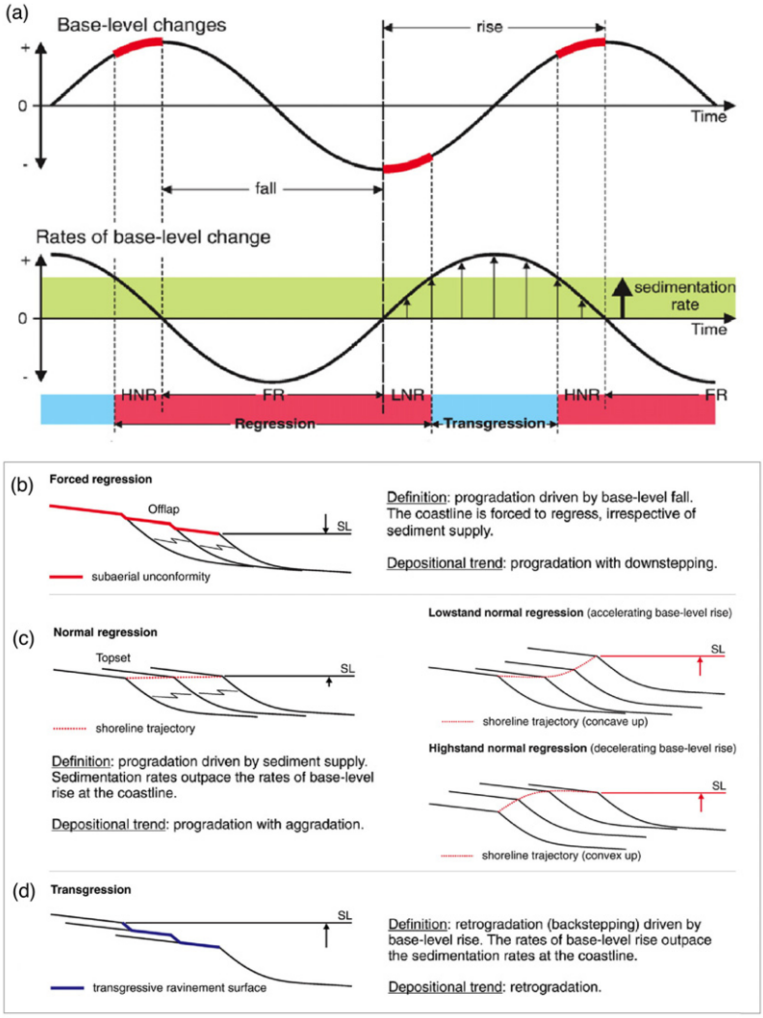

Fig. 4. Genetic types of stratal stacking patterns as a function of changes in relative sea level. In (a), sediment supply is assumed to be constant, as pointed by the shaded green area. The upper curve corresponds to base-level (sea-level changes) and the lower curve corresponds to the rate of sea-level change. The corresponding arrangement of strata for forced regression, normal regression (both lowstand and highstand) and transgression are depicted respectively in (b), (c), and (d). Adapted from [6,7].

of the network. A synchronizing event operates over $n \geq 2$ automata, triggering n simultaneous transitions, one per automaton. Each event in a SAN model has an occurrence rate, which can be constant or a function of other automata current states. Also, for each possible transition of a same event there is a choice or routing probability. Again, the event routing probability can be constant or functional.

A SAN model is defined by its *Markovian descriptor*, a compact algebraic expression composed of tensor operations over the matrices representing each automaton on the network. This compact representation of SAN enables memory savings, since storing some small matrices (of the order of each automaton) requires less memory usage than storing the infinitesimal generator itself. In addition, the tensor format of SAN enables the use of specialized algorithms [2,12,13,14] which are more efficient

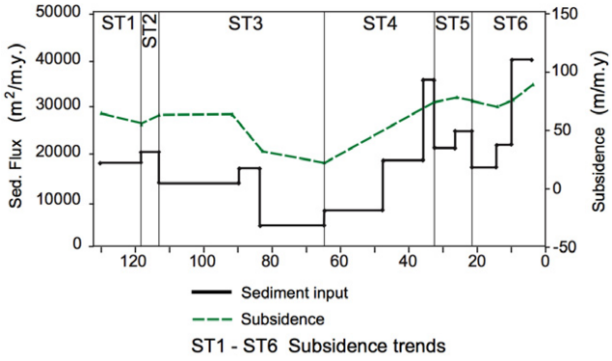

Fig. 5. Estimates of subsidence and sediment input rates for the past 130 Ma for Pelotas basin based on numerical modeling. Reproduced from [4].

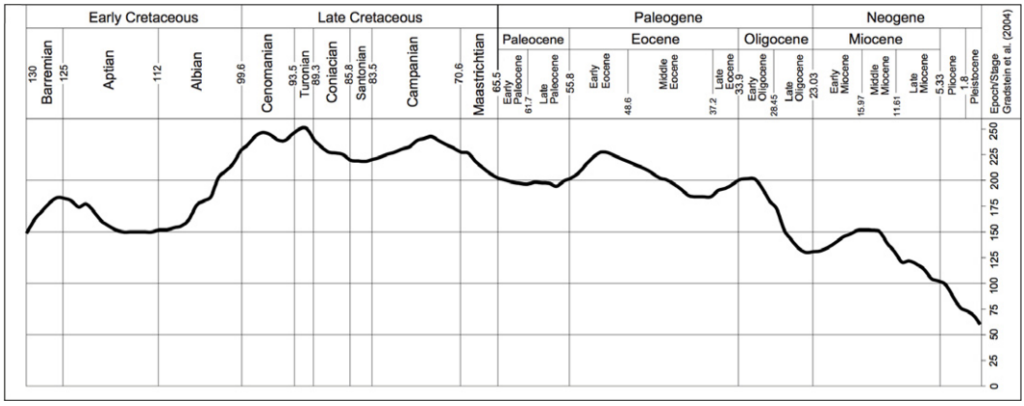

Fig. 6. Second order eustatic sea-level curve from Hardenbol *et al.* [11], re-calibrated according to Gradstein *et al.* [9] geologic timescale as proposed by Contreras [10].

than those used for solving large Markov chains.

For readers interested in further details on SAN, such as the formalism origin, improvements, classical and generalized tensor algebra, besides the material already referred, the following works are suggested [15,3,16]. Those interested in further modeling examples using SAN can find extensive material in [17,18,19,20,21,22,23,24].

3.1 Example: Heads or Tails

Heads or Tails is a coin-tossing game with a series of known variations. The one presented here has one coin and one player. At each coin flip, the player must guess which side will come with the face up. The player wins whenever his expectation is confirmed, otherwise he loses.

Figure 7 presents a possible SAN model for this problem. It has two automata: one representing the player's guess (automaton P), which is either *heads* or *tails*; and the other representing a tossing engine (automaton C), which is capable of tossing the coin and computing the outcome.

Automaton P has two states: "H" and "T". Routing probabilities π_{PH} and π_{PT} indicate the player guesses, being the probability of choosing heads and tails,

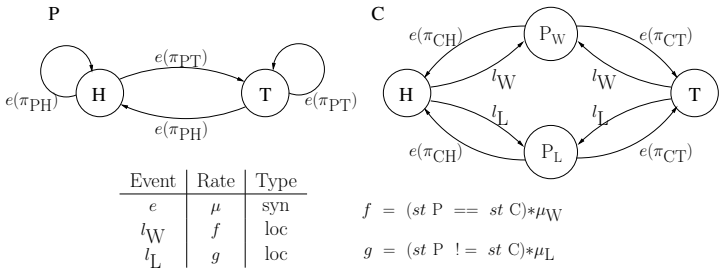

Fig. 7. Heads or Tails – SAN Modeling.

respectively. Automaton C has four states: "H" and "T", indicating the actual result of the coin-tossing; "P_W" (player wins) for the case the result matches the player's guess and "P_L" (player loses) otherwise. The coin has probabilities π_{CH} and π_{CT} of coming with the heads or tails side up, respectively, as the toss result.

The coin-tossing and the player's guess are simultaneous, represented by a synchronizing event, e, which triggers transitions leading to "H" or "T" in both automata. Such event can only happen when each automaton is in condition to attend it, which means automaton C must be either in "P_W" or "P_L".

As soon as the synchronizing event e happens, it follows a verification of whether the player has won or lost the match. Depending on the result, either of the local events on automaton C is triggered: event "l_W" leads to state "P_W" (player wins), while event "l_L" leads to state "P_L" (player loses).

4 SAN Model for the Pelotas Basin Strata Configuration

This section presents a SAN model developed for predicting the types of stratal stacking patterns expected for Pelotas Basin along the past 130 Ma.

As seen on Section 2, there are four types of deposit respectively associated to forced regression (FR), lowstand normal regression (LNR), highstand normal regression (HNR) and transgression (T). The first one occurs whenever the relative sea level falls. The other three distinguish from one another by the relative contribution of relative sea level rise rate and sediment supply rate. Note that the relative sea level is a function of the global (*eustatic*) sea level and crustal vertical movement. In our study case, there is no uplift and all the vertical movement is downwards, *i.e. subsidence*.

In this scenario it is possible to identify four important measures as the starting point for modeling, corresponding to the variation rates of: (1) eustatic sea level (ESL); (2) subsidence (S); (3) relative sea level (RSL); and (4) sediment supply (SS). Each of these four measures corresponds to one automaton in Figure 8, whose states were conceived based on a cluster of values achieved by Contreras *et al.* [4]. This figure also presents one automaton for time tracking and four other automata for restricting the model behavior. The model complete description is given by Figure 8 together with Table 4 and Table 3, being the first table the one responsible for providing the automata semantics and the last for listing the events and their

rates.

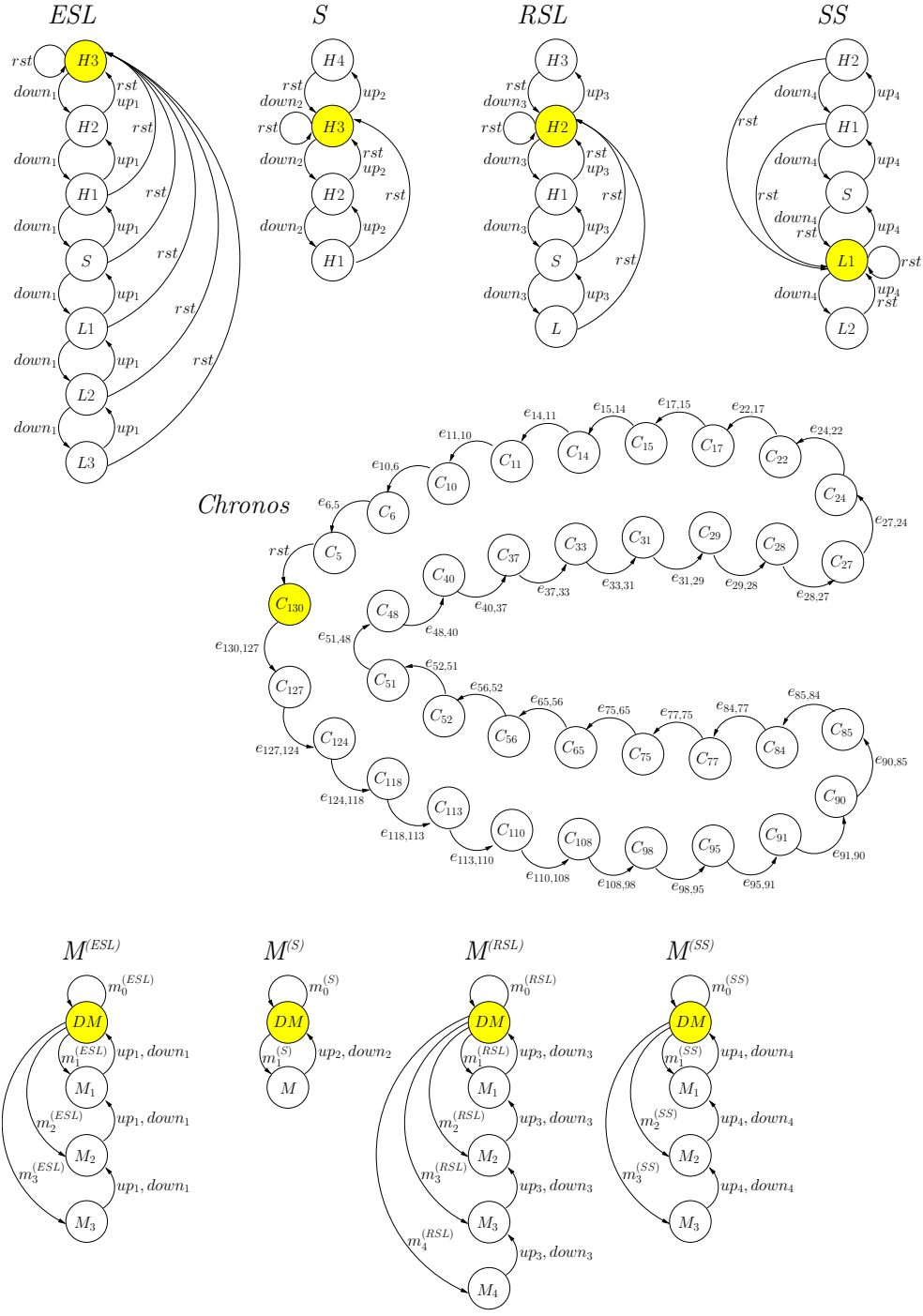

Fig. 8. Pelotas Basin - Automata of the SAN Model.

Figure 8 highlights the set of starting states in this model. Note that *Chronos* $= C_{130}$ is the starting point in time. It represents the time period between 130 Ma

Table 1
The semantic of automata of the proposed model.

ESL	Automaton indicating changes in the global (eustatic) sea level rate. State "*S*" stands for "standard", states "*H*" stand for "high" and states "*L*" stand for "low", such that the rate rises in accordance with the sequence $\{L_3 \dots H_3\}$.
S	Automaton indicating changes in the subsidence rate. States "*H*" stand for "high", such that the rate rises in accordance with the sequence $\{H_1 \dots H_4\}$.
RSL	Automaton indicating changes in the local (relative) sea level rate. State "*S*" stands for "standard", states "*H*" stand for "high" and state "*L*" stands for "low", such that the rate rises in accordance with the sequence $\{L \dots H_3\}$.
SS	Automaton indicating changes in the sediment supply rate. State "*S*" stands for "standard", states "*H*" stand for "high" and states "*L*" stand for "low", such that the value rises in accordance with the sequence $\{L_2 \dots H_2\}$.
Chronos	Automaton indicating this study timeline, from 130 million years ago to present time. States "*C*" stand for "Chronos".
$M^{(ESL)}$	Associated to automaton *ESL*, this automaton works as a semaphore, enabling *ESL* to change its state. State "*DM*" stands for "don't move" and states "*M*" stand for "move", such that the number of steps to move is given by the state index. For example: M_2 indicates two steps.
$M^{(S)}$	Associated to automaton *S*, this automaton works as a semaphore, enabling *S* to change its state. State "*DM*" stands for "don't move" and state "*M*" stands for "move one step forward".
$M^{(RSL)}$	Associated to automaton *RSL*. This automaton works as a semaphore, enabling *RSL* to change its state. State "*DM*" stands for "don't move" and states "*M*" stand for "move", such that the number of steps to move is given by the state index. For example: M_2 indicates two steps.
$M^{(SS)}$	Associated to automaton *SS*, this automaton works as a semaphore, enabling *SS* to change its state. State "*DM*" stands for "don't move" and states "*M*" stand for "move", such that the number of steps to move is given by the state index. For example: M_2 indicates two steps.

and 127 Ma, which comprises a time interval of 3 Ma. The state C_{130} is followed by the state C_{127}, such that the frequency associated to this transition is of one departure every 3 Ma, which corresponds to the rate of this event: $e_{130,127} = 0.3333$ (see Table 3). State C_{127} comprises the period between 127 Ma and 124 Ma, giving an event rate of $e_{127,124} = 0.3333$, coincidentially the same as before. State C_{124} comprises the period between 124 Ma and 118 Ma, with an event rate of $e_{124,118} = 0.1667$, that is, the state C_{124} is left in a proportion of one departure every 6 Ma.

Additionally, each event of time passage (events of automaton *Chronos*) triggers synchronous transitions on automata $M^{(ESL)}$, $M^{(S)}$, $M^{(RSL)}$ and $M^{(SS)}$. In order to favor clarity, the M automata have the transitions leaving the *DM* states labeled by groupings (first column of Table 3). For instance, label $m_0^{(ESL)}$ is used to refer to transitions in automaton *ESL* due to any of these events: $e_{118,113}$, $e_{91,90}$, $e_{51,48}$, $e_{17,15}$, *rst*.

At Table 3, event $e_{130,127}$ is assigned to labels $m_3^{(ESL)}$, $m_0^{(S)}$, $m_1^{(RSL)}$, $m_0^{(SS)}$. Looking for these labels in the M automata one comprehends that the transition from C_{130} to C_{127} happens simultaneously to the transitions leading from *DM* to M_3 in automaton $M^{(ESL)}$, leading back to *DM* in automaton $M^{(S)}$, to M_1 in automaton $M^{(RSL)}$ and leading back to *DM* in automaton $M^{(SS)}$.

In this new configuration, after synchronous transitions in *Chronos* and the M automata have taken place, only two kinds of events are possible: the *up* and *down* events. These events are also synchronizing ones, such that transitions in automaton $M^{(XYZ)}$ are accompanied by transitions in automaton *XYZ* (where *XYZ* refers to the automata *ESL*, *S*, *RSL* and *SS*), in the sense that the *up* events lead to higher

Table 2
The events and their rates for the proposed model.

Label	Event	Rate	Type
$m_3^{(ESL)}, m_0^{(S)}, m_1^{(RSL)}, m_0^{(SS)}$	$e_{130,127}$	0.3333	sync
$m_0^{(ESL)}, m_1^{(S)}, m_0^{(RSL)}, m_1^{(SS)}$	$e_{51,48}$	0.3333	sync
$m_1^{(ESL)}, m_1^{(S)}, m_4^{(RSL)}, m_0^{(SS)}$	$e_{127,124}$	0.3333	sync
$m_1^{(ESL)}, m_1^{(S)}, m_1^{(RSL)}, m_0^{(SS)}$	$e_{48,40}$	0.1250	sync
$m_1^{(ESL)}, m_0^{(S)}, m_1^{(RSL)}, m_1^{(SS)}$	$e_{124,118}$	0.1667	sync
$m_1^{(ESL)}, m_0^{(S)}, m_2^{(RSL)}, m_3^{(SS)}$	$e_{40,37}$	0.3333	sync
$m_0^{(ESL)}, m_1^{(S)}, m_2^{(RSL)}, m_1^{(SS)}$	$e_{118,113}$	0.2000	sync
$m_1^{(ESL)}, m_0^{(S)}, m_1^{(RSL)}, m_2^{(SS)}$	$e_{37,33}$	0.2500	sync
$m_1^{(ESL)}, m_0^{(S)}, m_1^{(RSL)}, m_0^{(SS)}$	$e_{113,110}$	0.3333	sync
$m_2^{(ESL)}, m_0^{(S)}, m_1^{(RSL)}, m_0^{(SS)}$	$e_{33,31}$	0.5000	sync
$m_1^{(ESL)}, m_0^{(S)}, m_2^{(RSL)}, m_0^{(SS)}$	$e_{110,108}$	0.5000	sync
$m_2^{(ESL)}, m_0^{(S)}, m_2^{(RSL)}, m_0^{(SS)}$	$e_{31,29}$	0.5000	sync
$m_2^{(ESL)}, m_0^{(S)}, m_2^{(RSL)}, m_0^{(SS)}$	$e_{108,98}$	0.1000	sync
$m_3^{(ESL)}, m_1^{(S)}, m_1^{(RSL)}, m_0^{(SS)}$	$e_{29,28}$	1.0000	sync
$m_1^{(ESL)}, m_1^{(S)}, m_0^{(RSL)}, m_0^{(SS)}$	$e_{98,95}$	0.3333	sync
$m_2^{(ESL)}, m_0^{(S)}, m_0^{(RSL)}, m_1^{(SS)}$	$e_{28,27}$	1.0000	sync
$m_2^{(ESL)}, m_0^{(S)}, m_0^{(RSL)}, m_0^{(SS)}$	$e_{95,91}$	0.2500	sync
$m_1^{(ESL)}, m_0^{(S)}, m_1^{(RSL)}, m_0^{(SS)}$	$e_{27,24}$	0.3333	sync
$m_0^{(ESL)}, m_0^{(S)}, m_1^{(RSL)}, m_0^{(SS)}$	$e_{91,90}$	1.0000	sync
$m_1^{(ESL)}, m_1^{(S)}, m_1^{(RSL)}, m_2^{(SS)}$	$e_{24,22}$	0.5000	sync
$m_1^{(ESL)}, m_1^{(S)}, m_1^{(RSL)}, m_1^{(SS)}$	$e_{90,85}$	0.2000	sync
$m_1^{(ESL)}, m_0^{(S)}, m_2^{(RSL)}, m_0^{(SS)}$	$e_{22,17}$	0.2000	sync
$m_1^{(ESL)}, m_0^{(S)}, m_0^{(RSL)}, m_0^{(SS)}$	$e_{85,84}$	1.0000	sync
$m_0^{(ESL)}, m_0^{(S)}, m_1^{(RSL)}, m_1^{(SS)}$	$e_{17,15}$	0.5000	sync
$m_1^{(ESL)}, m_0^{(S)}, m_1^{(RSL)}, m_0^{(SS)}$	$e_{84,77}$	0.1429	sync
$m_1^{(ESL)}, m_0^{(S)}, m_0^{(RSL)}, m_0^{(SS)}$	$e_{15,14}$	1.0000	sync
$m_1^{(ESL)}, m_0^{(S)}, m_1^{(RSL)}, m_0^{(SS)}$	$e_{77,75}$	0.5000	sync
$m_1^{(ESL)}, m_0^{(S)}, m_3^{(RSL)}, m_0^{(SS)}$	$e_{14,11}$	0.3333	sync
$m_1^{(ESL)}, m_0^{(S)}, m_1^{(RSL)}, m_0^{(SS)}$	$e_{75,65}$	0.1000	sync
$m_1^{(ESL)}, m_1^{(S)}, m_3^{(RSL)}, m_2^{(SS)}$	$e_{11,10}$	1.0000	sync
$m_2^{(ESL)}, m_0^{(S)}, m_0^{(RSL)}, m_0^{(SS)}$	$e_{65,56}$	0.1111	sync
$m_1^{(ESL)}, m_0^{(S)}, m_0^{(RSL)}, m_0^{(SS)}$	$e_{10,6}$	0.2500	sync
$m_2^{(ESL)}, m_0^{(S)}, m_1^{(RSL)}, m_0^{(SS)}$	$e_{56,52}$	0.2500	sync
$m_1^{(ESL)}, m_0^{(S)}, m_0^{(RSL)}, m_0^{(SS)}$	$e_{6,5}$	1.0000	sync
$m_1^{(ESL)}, m_0^{(S)}, m_2^{(RSL)}, m_0^{(SS)}$	$e_{52,51}$	1.0000	Type
$m_0^{(ESL)}, m_0^{(S)}, m_0^{(RSL)}, m_0^{(SS)}$	rst	0.2000	sync

Event	Rate	Type	Event	Rate	Type
up_1	f_{up_1}	sync	$down_1$	f_{down_1}	sync
up_2	f_{up_2}	sync	$down_2$	f_{down_2}	sync
up_3	f_{up_3}	sync	$down_3$	f_{down_3}	sync
up_4	f_{up_4}	sync	$down_4$	f_{down_4}	sync

rates[4] in the *XYZ* automaton, while the *down* events force the rate to low down. Although both kinds of events are predicted in the model, it is expected that only one per automaton is enabled at a moment. The functions enabling and disabling the *up* and *down* events are the f_{up_x} and f_{down_x} functions (where x assumes an index

[4] Note that automata *ESL*, *S*, *RSL*, *SS* are composed of states representing *rates* of the physical phenomena modeled. These rates are unrelated to the rates of the events themselves.

Table 3
The events and their rates for the proposed model (cont'd).

f_{up_1}	=	(	$(st\ Chronos == C_6)$	$\|\|$	$(st\ Chronos == C_{11})$	$\|\|$	$(st\ Chronos == C_{22})$	$\|\|$		
			$(st\ Chronos == C_{24})$	$\|\|$	$(st\ Chronos == C_{27})$	$\|\|$	$(st\ Chronos == C_{29})$	$\|\|$		
			$(st\ Chronos == C_{37})$	$\|\|$	$(st\ Chronos == C_{40})$	$\|\|$	$(st\ Chronos == C_{56})$	$\|\|$		
			$(st\ Chronos == C_{65})$	$\|\|$	$(st\ Chronos == C_{84})$	$\|\|$	$(st\ Chronos == C_{85})$	$\|\|$		
			$(st\ Chronos == C_{95})$	$\|\|$	$(st\ Chronos == C_{108})$	$\|\|$	$(st\ Chronos == C_{110})$	$\|\|$		
			$(st\ Chronos == C_{118})$	$) * 1000$						
f_{down_1}	=	(	$(st\ Chronos == C_5)$	$\|\|$	$(st\ Chronos == C_{10})$	$\|\|$	$(st\ Chronos == C_{14})$	$\|\|$		
			$(st\ Chronos == C_{17})$	$\|\|$	$(st\ Chronos == C_{28})$	$\|\|$	$(st\ Chronos == C_{31})$	$\|\|$		
			$(st\ Chronos == C_{33})$	$\|\|$	$(st\ Chronos == C_{51})$	$\|\|$	$(st\ Chronos == C_{52})$	$\|\|$		
			$(st\ Chronos == C_{75})$	$\|\|$	$(st\ Chronos == C_{77})$	$\|\|$	$(st\ Chronos == C_{91})$	$\|\|$		
			$(st\ Chronos == C_{98})$	$\|\|$	$(st\ Chronos == C_{124})$	$\|\|$	$(st\ Chronos == C_{127})$	$) * 1000$		
f_{up_2}	=	(	$(st\ Chronos == C_{10})$	$\|\|$	$(st\ Chronos == C_{28})$	$\|\|$	$(st\ Chronos == C_{40})$	$\|\|$		
			$(st\ Chronos == C_{48})$	$\|\|$	$(st\ Chronos == C_{113})$	$) * 1000$				
f_{down_2}	=	(	$(st\ Chronos == C_{22})$	$\|\|$	$(st\ Chronos == C_{85})$	$\|\|$	$(st\ Chronos == C_{95})$	$\|\|$		
			$(st\ Chronos == C_{124})$	$) * 1000$						
f_{up_3}	=	(	$(st\ Chronos == C_{11})$	$\|\|$	$(st\ Chronos == C_{15})$	$\|\|$	$(st\ Chronos == C_{27})$	$\|\|$		
			$(st\ Chronos == C_{29})$	$\|\|$	$(st\ Chronos == C_{33})$	$\|\|$	$(st\ Chronos == C_{40})$	$\|\|$		
			$(st\ Chronos == C_{51})$	$\|\|$	$(st\ Chronos == C_{65})$	$\|\|$	$(st\ Chronos == C_{85})$	$\|\|$		
			$(st\ Chronos == C_{90})$	$\|\|$	$(st\ Chronos == C_{110})$	$\|\|$	$(st\ Chronos == C_{113})$	$\|\|$		
			$(st\ Chronos == C_{118})$	$) * 1000$						
f_{down_3}	=	(	$(st\ Chronos == C_{10})$	$\|\|$	$(st\ Chronos == C_{17})$	$\|\|$	$(st\ Chronos == C_{22})$	$\|\|$		
			$(st\ Chronos == C_{28})$	$\|\|$	$(st\ Chronos == C_{31})$	$\|\|$	$(st\ Chronos == C_{37})$	$\|\|$		
			$(st\ Chronos == C_{52})$	$\|\|$	$(st\ Chronos == C_{75})$	$\|\|$	$(st\ Chronos == C_{77})$	$\|\|$		
			$(st\ Chronos == C_{98})$	$\|\|$	$(st\ Chronos == C_{108})$	$\|\|$	$(st\ Chronos == C_{124})$	$) * 1000$		
f_{up_4}	=	(	$(st\ Chronos == C_{10})$	$\|\|$	$(st\ Chronos == C_{15})$	$\|\|$	$(st\ Chronos == C_{27})$	$\|\|$		
			$(st\ Chronos == C_{37})$	$\|\|$	$(st\ Chronos == C_{48})$	$\|\|$	$(st\ Chronos == C_{118})$	$) * 1000$		
f_{down_4}	=	(	$(st\ Chronos == C_{22})$	$\|\|$	$(st\ Chronos == C_{33})$	$\|\|$	$(st\ Chronos == C_{85})$	$\|\|$		
			$(st\ Chronos == C_{113})$	$) * 1000$						

in the set $x = \{1, 2, 3, 4\}$), which depend only on the *Chronos* current state. Some tests were executed in order to choose a rate for the *up* and *down* events and, as observed, setting these events rate to arround 1000 fits better to the results expected from Contreras *et al.* [4]. The transitions only cease when every M automaton reach state *DM*, disabling the *up* and *down* events and enabling once again the next event synchronizing a transition in *Chronos* with a transition in each of the M automata.

Event *rst*, a short for *reset*, is the only one in the whole model that synchronizes transitions between all the automata, restoring the model to its starting point configuration, back in 130 Ma.

5 Experiment and Results

It is usual to conduct a modeling activity in order to obtain probability measures for some given reality. In this study, the measures of interest are obtained by means of *integration functions*, which are mathematical expressions for selecting the exact information to inspect.

Here, the integration functions represent the four types of deposit or configuration strata: *T*, *FR*, *LNR* and *HNR*, as discussed in Section 2. These types of deposit are strongly dependent on the relative sea level rate and the sediment supply rate, represented respectively by the automata *RSL* and *SS* (see Figure 8). Direct de-

pendencies on the eustatic (global) sea level and subsidence, automata *ESL* and *S*, respectively, are subtle but yet taken into account, since they bring more realism to the model.

All possible configurations previously described are combined in order to build one function per configuration strata per *Chronos* state. As an example to be generalized to other states of *Chronos*, Table 4 presents the integration functions built for state C_{130}.

Table 4
Integration functions for the Pelotas Basin model, considering state C_{130}.

T_C_{130}	$= ((st\ Chronos == C_{130})\ \&\&$ $(\ ((st\ RSL == H_3)\ \&\&\ ((st\ SS == L_1)\ \|\|\ (st\ SS == L_2)))\ \|\|$ $((st\ RSL == H_2)\ \&\&\ (st\ SS == L_2))\ \|\|$ $((st\ RSL == H_1)\ \&\&\ (st\ SS == L_2))$ $));$
HNR_C_{130}	$= ((st\ Chronos == C_{130})\ \&\&\ (f_{down_3})\ \&\&$ $(\ ((st\ RSL == H_1)\ \&\&\ (st\ SS == H_2))\ \|\|$ $((st\ RSL == S)\ \ \&\&\ (st\ SS == H_2))\ \|\|$ $((st\ RSL == S)\ \ \&\&\ (st\ SS == H_1))$ $));$
LNR_C_{130}	$= ((st\ Chronos == C_{130})\ \&\&\ (f_{up_3})\ \&\&$ $(\ ((st\ RSL == H_1)\ \&\&\ (st\ SS == H_2))\ \|\|$ $((st\ RSL == S)\ \ \&\&\ (st\ SS == H_2))\ \|\|$ $((st\ RSL == S)\ \ \&\&\ (st\ SS == H_1))$ $));$
FR_C_{130}	$= ((st\ Chronos == C_{130})\ \&\&\ (st\ RSL == L_1));$

Considering the distribution of configuration strata along the past 130 Ma obtained by this modeling activity, the goal of this experiment is to validate the model by comparing the achieved results with those presented by Contreras *et al.* [4]. Furthermore, the way this model was developed, it is possible to predict the probability of each type of deposit within the same *Chronos* state.

Then, summarizing, there are basically four different types of deposit, as discussed in Section 2: forced regression (*FR*), lowstand normal regression (*LNR*), highstand normal regression (*HNR*) and transgression (*T*). Table 5 confronts information on these stratal patterns obtained by Contreras *et al.* [4] with the results achieved by the SAN model for Pelotas Basin (see Figure 8, Table 4 and Table 3).

Observing Table 5 in detail, the first three columns respectively present the time period in millions of years, the relative sea level rate and the sediment supply rate. The fourth column presents Contreras *et al.* [4] estimates based on the interpretation of the sedimentary record. Under the "probabilities" grouping are the columns displaying the probabilities obtained by solving the SAN model for Pelotas Basin. In order to ease the analysis, the last column in this table provides a quick summary on this experiment expectations. Signal † indicates a mismatch between the estimate and the result obtained by solving the model with the specified integration functions (as an example, see Table 4); signal ✓ indicates a match.

Important to mention that among the existing tools for solving SAN mod-

Table 5
Expected and Achieved Results

time period (Ma)	relative sea level rate	sediment supply rate	Contreras *et al.* 2010	probabilities				match
				T	HNR	LNR	FR	
130 - 127	77	18000		**1.0000**	0.0000	0.0000	0.0000	
127 - 124	62	18000		**1.0000**	0.0000	0.0000	0.0000	
124 - 118	54	18000		0.0005	0.0001	0.0000	**0.9994**	
118 - 113	55	20000		0.0000	**0.7339**	0.2660	0.0001	
113 - 110	67	14500		**0.9996**	0.0000	0.0004	0.0000	
110 - 108	70	14500	T	**1.0000**	0.0000	0.0000	0.0000	✓
108 - 98	73	14500	T	**1.0000**	0.0000	0.0000	0.0000	✓
98 - 95	63	14500		0.0003	0.0002	0.0000	**0.9995**	
95 - 91	64	14500		0.0000	0.0000	0.0000	**1.0000**	
91 - 90	43	14500		0.0000	0.0000	0.0000	**1.0000**	
90 - 85	43	17000		0.0000	0.0000	**0.9997**	0.0003	
85 - 84	40	5000		**0.9995**	0.0000	0.0005	0.0000	
84 - 77	43	5000	T	**1.0000**	0.0000	0.0000	0.0000	✓
77 - 75	36	5000		0.0012	**0.9998**	0.0000	0.0000	
75 - 65	26	5000		0.0000	0.0000	0.0000	**1.0000**	
65 - 56	30	8500		0.0000	0.0000	**0.9997**	0.0003	
56 - 52	48	8500	FR	0.0000	0.0000	**1.0000**	0.0000	†
52 - 51	40	8500		0.0000	0.0004	0.0000	**0.9996**	
51 - 48	41	8500	T	**0.9995**	0.0000	0.0001	0.0003	✓
48 - 40	53	19000	T	**1.0000**	0.0000	0.0000	0.0000	✓
40 - 37	65	19000		**1.0000**	0.0000	0.0000	0.0000	
37 - 33	74	36000	HNR	0.0003	**0.9997**	0.0000	0.0000	✓
33 - 31	75	21000	LNR	**0.7993**	0.0000	0.2007	0.0000	†
31 - 29	63	21000		0.0005	**0.9995**	0.0000	0.0000	
29 - 28	72	21000		**0.9997**	0.0000	0.0021	0.0000	
28 - 27	49	21000	T	**0.8000**	0.2000	0.0000	0.0000	✓
27 - 24	73	25000		**0.6000**	0.0000	0.4000	0.0000	
24 - 22	81	25000	HNR	0.4001	**0.5999**	0.0000	0.0000	✓
22 - 17	79	17000		**0.9998**	0.0002	0.0000	0.0000	
17 - 15	75	17000		0.0005	0.0003	0.0000	**0.9992**	
15 - 14	70	22000	LNR	0.0000	0.0000	**0.9987**	0.0013	✓
14 - 11	61	22000		0.0000	0.0000	**1.0000**	0.0000	
11 - 10	75	22000	T	**0.9990**	0.0000	0.0010	0.0000	✓
10 - 6	74	41000		0.0003	**0.9997**	0.0000	0.0000	
6 - 5	90	41000		0.0000	**1.0000**	0.0000	0.0000	
5 - 0	82	41000	HNR	0.0000	0.0000	**1.0000**	0.0000	†

T	Transgression
FR	Forced Regression
LNR	Lowstand Normal Regression
HNR	Highstand Normal Regression

✓	Match between the model result and Contreras *et al.* 2010
†	Mismatch between the model result and Contreras *et al.* 2010

els [25,26], *SAN Lite-Solver* [27] was the one chosen for this research. The time required for solving the model presented in this paper (see Figure 8, Table 4 and Table 3) is not really significant, the order of a few seconds, being irrelevant for this paper analysis.

6 Discussion

This article presents a novel modeling case to represent specific geological phenomena. More precisely, this paper seeks for predicting generic types of stratal stacking patterns for Pelotas Basin. The major goal here is to illustrate a potentially useful and previously unknown prediction tool to estimate statistics about a natural phenomenon.

As seen in Table 5, the values obtained by the experiment (columns under the "probabilities" grouping) were relatively close to the Contreras *et al.* [4] classification. Ten out of the thirteen time intervals defined by Contreras matched exactly. The observed discrepancies were expected in the sense that this is a humble (but not least interesting) first attempt on using SAN modeling in a knowledge area as complex as geology, with too many factors to consider. These discrepancies are particularly interesting given that geological prediction approaches are usually based on a very different kind of research following punctual and restrictive analysis, such as drilling and seismic surveys, instead of a systematic approach brought by a stochastic modeling effort.

The three values that did not match may be explained by factors such as the granularity of the model compared with the timescale of the geological events considered. In the case of the mismatch for the time period comprised between 56 and 52 Ma, when Contreras et al. attribute a FR and our model predicts a LNR, we see that for the immediately following time period (52-51 Ma) we do expect a FR with 99.96% confidence. Note that 1 Ma is the minor time slice that we consider. The discrepancy in the 5-0 Ma time slot seems similar, since the model prediction for the 6-5 Ma time slot is the HNR situation estimated by Contreras *et al.* [4]. However, our prediction is a clear LNR situation (100%). Therefore, it is our belief that a granularity issue is causing the discrepancy as for the 56-52 Ma case. The last mismatch was found in the 33-31 Ma time slot. In this case our model returns probabilities of nearly 20% for LNR and 80% for TR, even though Contreras' prediction clearly state a LNR situation. Maybe this discrepancy is related to a lack of detail in the model, but a further geological study is necessary to analyze the reasons of this case.

We believe that this paper research is valuable not only by the subject itself, but also by the challenge it represents. It is always difficult to work in a multidisciplinary endeavor, where collaborators must learn how to communicate. Thus, the natural next step in this research is to refine this model, enriching with data from alternative literature allied to the knowledge obtained from this preliminary work.

Nevertheless, the proposed model represents a contribution by itself, since it offers unusual complex modeling primitives as the automata $M^{(ESL)}$, $M^{(S)}$, $M^{(RSL)}$, and $M^{(SS)}$ used to represent a memory notion to the changes in the automata *ESL*, *S*, *RSL*, and *SS*, respectively, according to the passage of time expressed in automaton *Chronos*.

Finally, this practical application of the SAN modeling brings up new opportunities to the Stochastic Modeling area. Perhaps one of the most notable benefits

of using stochastic modeling to depict a natural phenomenon is that statistics generated can help against major human error factors that may arise with classical geological analysis. Anyway, this is our bet for continuing doing such multidisciplinary research.

References

[1] B. Plateau, On the stochastic structure of parallelism and synchronization models for distributed algorithms, ACM SIGMETRICS Performance Evaluation Review 13 (1985) 147–154.

[2] P. Fernandes, B. Plateau, W. J. Stewart, Efficient descriptor-vector multiplication in Stochastic Automata Networks, Journal of the ACM 45 (1998) 381–414.

[3] L. Brenner, P. Fernandes, A. Sales, The Need for and the Advantages of Generalized Tensor Algebra for Kronecker Structured Representations, International Journal of Simulation: Systems, Science & Technology (IJSIM) 6 (2005) 52–60.

[4] J. Contreras, R. Zühlke, S. Bowman, T. Bechstädt, Seismic stratigraphy and subsidence analysis of the Southern Brazilian margin (Campos, Santos and Pelotas basins), Marine and Petroleum Geology 27 (2010) 1952–1980.

[5] H. Posamentier, M. Jervey, P. Vail, C. Wilgus, B. Hastings, C. St Kendall, C. Ross, J. Van Wagoner, Eustatic controls on clastic deposition i - conceptual framework, in: Sea-Level Changes: An Integrated Approach, volume 42 of *Soc. of Econ. Paleontologists and Mineralogists. Special Publication Series*, Books on Demand, 1988, pp. 109–124.

[6] O. Catuneanu, Principles of Sequence Stratigraphy, Elsevier, Amsterdam, 2006.

[7] O. Catuneanu, V. Abreu, J. Bhattacharya, M. Blum, R. Dalrymple, P. Eriksson, C. Fielding, W. Fisher, W. Galloway, M. Gibling, K. Giles, J. Holbrook, R. Jordan, C. Kendall, B. Macurda, O. Martinsen, A. Miall, J. Neal, D. Nummedal, L. Pomar, H. Posamentier, B. Pratt, J. Sarg, K. Shanley, R. Steel, A. Strasser, M. Tucker, C. Winker, Towards the standardization of sequence stratigraphy, Earth-Science Reviews 92 (2009) 1–33.

[8] J. Hardenbol, J. Thierry, M. Farley, T. Jacquin, P. de Graciansky, P. Vail, Mesozoic and Cenozoic sequence chronostratigraphic framework of European Basins, in: Mesozoic and Cenozoic Sequence Stratigraphy of European Basins, volume 60 of *Soc. of Econ. Paleontologists and Mineralogists. Special Publication Series*, 1998, pp. 3–13.

[9] F. Gradstein, J. Ogg, A. Smith, A Geologic Time Scale, 2005.

[10] J. Contreras, Seismo-stratigraphy and numerical basin modeling of the southern Brazilian continental margin (Campos, Santos, and Pelotas basins), Ph.D. thesis, Ruprecht-Karls-Universität, Heidelberg, Germany, 2011.

[11] J. Van Wagoner, H. Posamentier, R. Mitchum Jr., P. Vail, J. Sarg, T. Loutit, J. Hardenbol, An overview of the fundamentals of sequence stratigraphy and key definitions, in: Sea-Level Changes: An Integrated Approach, volume 42 of *Soc. of Econ. Paleontologists and Mineralogists. Special Publication Series*, Books on Demand, 1988, pp. 39–45.

[12] R. M. Czekster, P. Fernandes, J.-M. Vincent, T. Webber, Split: a flexible and efficient algorithm to vector-descriptor product, in: International Conference on Performance Evaluation Methodologies and tools (ValueTools'07), volume 321 of *ACM International Conferences Proceedings Series*, ACM Press, 2007, pp. 83–95.

[13] R. M. Czekster, P. Fernandes, T. Webber, Efficient vector-descriptor product exploiting time-memory trade-offs, ACM SIGMETRICS Performance Evaluation Review 39 (2011) 2–9. doi: 10.1145/2160803.2160805.

[14] A. M. Lima, M. A. Netto, T. Webber, R. M. Czekster, C. A. D. Rose, P. Fernandes, Performance evaluation of openmp-based algorithms for handling kronecker descriptors, Journal of Parallel and Distributed Computing 72 (2012) 678–692.

[15] P. Fernandes, Méthodes numériques pour la solution de systèmes Markoviens à grand espace détats, Ph.D. thesis, Institut National Polytechnique de Grenoble, Grenoble, France, 1998.

[16] T. Webber, Reducing the Impact of State Space Explosion in Stochastic Automata Networks, Ph.D. thesis, Pontifícia Universidade Católica do Rio Grande do Sul (PUCRS), Brasil, 2009.

[17] A. G. Farina, P. Fernandes, F. M. Oliveira, Representing software usage models with stochastic automata networks, in: Proceedings of the 14th International Conference on Software Engineering and Knowledge Engineering, SEKE '02, ACM, New York, NY, USA, 2002, pp. 401–407. doi: 10.1145/568760.568830.

[18] L. Baldo, L. Brenner, L. G. Fernandes, P. Fernandes, A. Sales, Performance Models For Master/Slave Parallel Programs, Electronic Notes in Theoretical Computer Science 128 (2005) 101–121. doi: 10.1016/j.entcs.2005.01.015.

[19] F. L. Dotti, P. Fernandes, A. Sales, O. M. Santos, Modular Analytical Performance Models for Ad Hoc Wireless Networks, in: Proceedings of the 3rd International Symposium on Modeling and Optimization in Mobile, Ad Hoc, and Wireless Networks (WiOpt 2005), IEEE Computer Society, 2005, pp. 164–173. doi: 10.1109/WIOPT.2005.31.

[20] R. Chanin, M. Corrêa, P. Fernandes, A. Sales, R. Scheer, A. F. Zorzo, Analytical Modeling for Operating System Schedulers on NUMA Systems, Electronic Notes in Theoretical Computer Science 151 (2006) 131–149. doi: 10.1016/j.entcs.2006.03.016.

[21] L. Brenner, P. Fernandes, J.-M. Fourneau, B. Plateau, Modelling Grid5000 point availability with SAN, Electronic Notes in Theoretical Computer Science 232 (2009) 165–178. doi: 10.1016/j.entcs.2009.02.056.

[22] F. L. Dotti, P. Fernandes, C. Nunes, Structured Markovian models for discrete spatial mobile node distribution, Journal of the Brazilian Computer Society 17 (2011) 31–52. doi: 10.1007/s13173-010-0026.

[23] P. Fernandes, A. Sales, A. R. Santos, T. Webber, Performance Evaluation of Software Development Teams: a Practical Case Study, Electronic Notes in Theoretical Computer Science 275 (2011) 73–92. doi: 10.1016/j.entcs.2011.09.006.

[24] R. M. Czekster, P. Fernandes, A. Sales, T. Webber, A. F. Zorzo, Stochastic Model for QoS Assessment in Multi-tier Web Services, Electronic Notes in Theoretical Computer Science 275 (2011) 53–72. doi: 10.1016/j.entcs.2011.09.005.

[25] A. Benoit, L. Brenner, P. Fernandes, B. Plateau, W. J. Stewart, The PEPS Software Tool, in: Computer Performance Evaluation (TOOLS 2003), volume 2794 of *LNCS*, Springer-Verlag Heidelberg, 2003, pp. 98–115.

[26] L. Brenner, P. Fernandes, B. Plateau, I. Sbeity, PEPS2007 - Stochastic Automata Networks Software Tool, in: Proceedings of the 4th International Conference on Quantitative Evaluation of SysTems (QEST 2007), IEEE Computer Society, Edinburgh, UK, 2007, pp. 163–164.

[27] A. Sales, San lite-solver: a user-friendly software tool to solve san models, in: Proceedings of the 2012 Symposium on Theory of Modeling and Simulation - DEVS Integrative M&S Symposium, TMS/DEVS '12, Society for Computer Simulation International, San Diego, CA, USA, 2012, pp. 44:9–16.